

LA-UR-17-29219

Approved for public release; distribution is unlimited.

Title: Second Order Tracking Verification for Unstructured Mesh in the MCNP[®] Code Post Version 6.2.0

Author(s): Roger L. Martz and Joel A. Kulesza

Intended For: General Reference / MCNP[®] Website

Issued: October 2017



Disclaimer: Los Alamos National Laboratory, an affirmative action/equal opportunity employer, is operated by the Los Alamos National Security, LLC for the National Nuclear Security Administration of the U.S. Department of Energy under contract DE-AC52-06NA25396. By approving this article, the publisher recognizes that the U.S. Government retains nonexclusive, royalty-free license to publish or reproduce the published form of this contribution, or to allow others to do so, for U.S. Government purposes. Los Alamos National Laboratory requests that the publisher identify this article as work performed under the auspices of the U.S. Department of Energy. Los Alamos National Laboratory strongly supports academic freedom and a researcher's right to publish; as an institution, however, the Laboratory does not endorse the viewpoint of a publication or guarantee its technical correctness.

This page intentionally left blank.

Second Order Tracking Verification for Unstructured Mesh in the MCNP[®] Code Post Version 6.2.0

Roger L. Martz and Joel A. Kulesza
Monte Carlo Methods, Codes, and Applications
X-Computational Physics Division
Los Alamos National Laboratory

October 2017

1 Introduction

The unstructured mesh (UM) capability in the Los Alamos National Laboratory (LANL) Monte Carlo N-Particle[®] (MCNP[®]) transport code has been under development since the mid-2000's [1]. This capability has been in every release of MCNP6 to the Radiation Safety Information Computational Center (RSICC) at Oak Ridge National Laboratory (ORNL) since the first beta release. Each MCNP release has provided improved UM features through scheduled code development, bug fixes, and integration with other code capabilities.

LANL staff have published many documents on the topic of UM. Most of these can be found on the MCNP website (mcnp.lanl.gov) under the Reference Collection. Anyone new to MCNP's UM capability should consider reading References 2 and 3.

After the 6.2.0 version release of MCNP6 was frozen for development, the surface intersection routines for the UM second order elements were examined and revised to be more robust. Coding was also improved to make it cleaner and more concise. This functionality will be available in future code releases.

The purpose of this report is to document verification that the code is producing correct results with second-order elements and to gain an understanding of performance when these elements are used. UM equivalents of four benchmark problems (two criticality and two fixed source) and one new analytical benchmark were examined for this purpose. In addition, a simple second-order UM geometry was constructed to compare the track length calculated as a result of UM tracking versus an analytic track length.

2 Background

The ability to track on an UM with second-order finite elements (tetrahedrons, pentahedrons, hexahedrons) has been in MCNP6 since the first beta release to RSICC. Since the beginning,

MCNP[®] and Monte Carlo N-Particle[®] are registered trademarks owned by Los Alamos National Security, LLC, manager and operator of Los Alamos National Laboratory. Any third party use of such registered marks should be properly attributed to Los Alamos National Security, LLC, including the use of the [®] designation as appropriate. Any questions regarding licensing, proper use, and/or proper attribution of Los Alamos National Security, LLC marks should be directed to trademarks@lanl.gov.

few models have been created at LANL with second-order elements. This was partly because of the success of models that used first-order elements. However, as users' comfort levels increase with a feature so does the need to increase model complexity with that feature to the point where computer memory limits start to become problematic and second-order elements will be needed to reduce the memory footprint. Consequently, little work was done early on to verify second-order elements.

The overwhelming benefit from using second-order elements is the curved nature of the element faces. Consequently, far fewer second-order elements are needed to accurately model parts constructed with curved surfaces. This translates to a smaller computer memory footprint for a model, compared to one with first-order elements. Many more (on the order to 10–100 times) first-order elements are generally needed to obtain accurate volumes for parts with curved surface.

The main downside to using second-order elements is that it is more computationally expensive to track particles with them. Generally, more-expensive iterative algorithms are needed to find intersection points with elemental faces. This is in contrast to the simpler direct solution of three simultaneous equations by matrix methods with first-order elements. In addition, the containment routines (finding a point in an element) require more floating point operations (FLOPs) because the complexity of the equations increase as the number of nodes per element increase when going from first to second order.

2.1 Benchmark Problem Descriptions

Four benchmark problems were chosen to verify second-order element tracking. Two problems were also used to examine the sensitivity of the results using various levels of mesh refinement. Two of these problems are criticality benchmarks from the International Handbook of Criticality Benchmark Experiments [4] and two are fixed-source benchmarks [5] performed at Lawrence Livermore National Laboratory (LLNL). In addition, a new analytic test problem was developed. These are briefly described next.

2.1.1 HEU-MET-FAST-001 : Simple Bare Sphere

One of the criticality experiments performed at LANL in the 1950's to determine the critical mass of a bare 94 wt.-% ^{235}U sphere of highly enriched uranium (HEU) consisted of two identical sets of nested oralloy hemispheres. The upper set was supported by a thick diaphragm of stainless steel; the lower set rested on a thin-wall aluminum cylinder. By remote control, the lower stack was raised to contact the steel diaphragm for each measurement of the multiplication of neutrons from a small near-central source.

Analysis of this experiment led to specification of the critical mass of a bare sphere of HEU termed "Lady Godiva." This was an example of a fast neutron critical system. It was a simple geometry, consisting of a 52.42-kg sphere of U (93.71), i.e., 93.71% U-235 enriched. The density of the system was measured at 18.74 g/cm³. These data correspond to a sphere of radius equal to 8.7407 cm. The criticality safety community has deemed this model as an acceptable benchmark [4].

2.1.2 IEU-MET-FAST-007 : Two-Zone Homogenized Model

This problem is an adaptation of the Big Ten critical benchmark 4. Big Ten was a large, mixed-uranium-metal, cylindrical core with 10% average ^{235}U enrichment surrounded by a thick ^{238}U reflector. The name “Big Ten” reflects both its total mass of uranium (10 metric tons) and the average ^{235}U enrichment of its core (10%).

A simplified two-zone homogenized model similar to the model of Big Ten used by the Cross Sections Evaluation Working Group (CSEWG) was developed on the detailed model (see Volume III, Section D.2 of Reference 4 where the assumptions for this model are detailed). For the current work, ENDF/B-VII cross sections were used. The models in this work were taken from Reference 6.

2.1.3 LLNL Pulsed Spheres

The LLNL pulsed sphere experiments consisted of time-of-flight spectrum measurements resulting from spheres of various materials pulsed with 14-MeV neutrons. Sometimes identical materials in different geometric configurations were used to investigate pulse spectrum behavior resulting from attenuation through various thicknesses of the material.

All spheres featured a channel through half of the sphere that permitted insertion of the target assembly used to produce the 14-MeV source neutrons. Assuming that the target assembly entered the sphere through the channel from the $+x$ direction, the detector package was positioned relative to the $-x$ direction. Note that the detector package was modeled as a ring detector within MCNP6 because of geometric and source symmetry. For each experiment, the detector was either a Pilot-B or NE213 scintillator and associated hardware, with the response functions given in Reference 7. When describing the spherical geometry, the dimensions were given in terms of 14-MeV neutron mean free paths (m.f.p.) along the flight path from the source to the detector to differentiate spheres using the same materials. Dimensions were also given in centimeters.

The two pulsed sphere models used herein were refactored from the Reference 8 work and are described below. The current work is an extension of some of the Reference 8 work. The solid models created in SpaceClaim were imported into Abaqus/CAE [9] and re-meshed with second-order elements. The results obtained with the second-order UM models of this work will be compared to the CSG results from Reference 8. The CSG calculations with the Detailed, Hybrid, and Legacy models were not repeated.

LLNL Beryllium Sphere The beryllium sphere with a thickness of 0.8 m.f.p. (outer radius of 12.58 cm) consisted of a spherical shell with a cylindrical channel and spherical hollow core as shown in Figure 1a. A Pilot-B detector with a 1.6-MeV cutoff energy and FWHM resolution of 4 ns was positioned 30 degrees off-axis with a flight-path distance of 765.2 cm. The detector captured results from 137 to 409 ns (corresponding to neutron energies of 1.8 to 16.7 MeV).

The CSG version of this problem exists in the MCNP validation suite with the problem identifier BE08 / lps_berl.

LLNL Water Sphere The water sphere with a thickness of 1.9 m.f.p. (outer radius of 22.55 cm) consisted of a spherical steel shell (0.15 cm) filled with water surrounded by another steel shell (0.06 cm) with a vacuum between both shells. Each shell had a tapered round channel leading to the center as shown in Figure 1b. A Pilot-B detector with a 1.6-MeV cutoff energy

and FWHM resolution of 5 ns is positioned 30 degrees off-axis with a flight-path distance of 754.0 cm. The detector captured results from 126 to 392 ns (corresponding to neutron energies of 1.9 to 19.3 MeV).

The CSG version of this problem exists in the MCNP validation suite with the problem identifier H2O19 / lps_water.

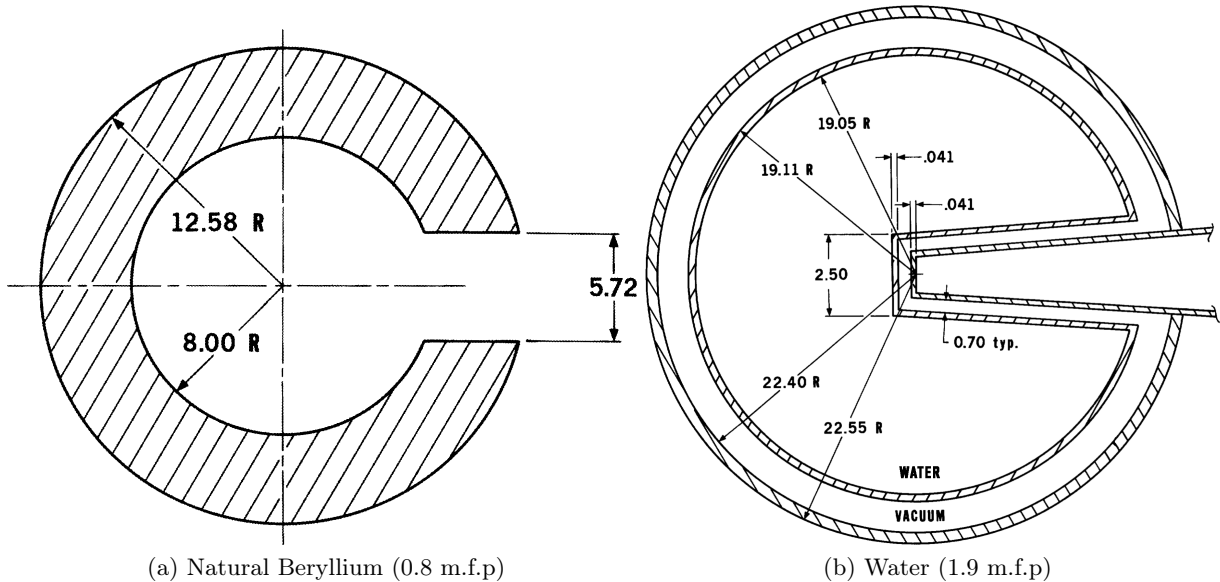


Figure 1: Pulsed sphere geometries reformatted from Reference [5] (dimensions are in units of centimeters).

2.2 Simple Problem Description

In addition to the aforementioned benchmark problems, a new geometry was created to compare the track length calculated as a result of UM tracking to an analytic calculation. This geometry also demonstrated the ability of second-order curved edges to preserve curvature and volume. The geometry (see Figure 2) consisted of a 2×2 -mesh region with the left edge concave and the right edge convex. This geometry was created in Abaqus by specifying the vertices at $(x, y) = (0, 0), (2, 0), (2, 2), (0, 2)$ and at $(0.5, 1)$ and $(2.5, 1)$. Straight edges were created from $(0, 0) \rightarrow (2, 0)$ and $(0, 2) \rightarrow (2, 2)$ with circular arcs created from $(0, 0) \rightarrow (0.5, 1) \rightarrow (0, 2)$ and $(2, 0) \rightarrow (2.5, 1) \rightarrow (2, 2)$. These arcs corresponded to circles with a radius of 1.25 cm centered at $(-0.75, 1)$ and $(1.25, 1)$, respectively.

This region was then extruded by 1 cm in the z direction (with the lower set of vertices at $z = 0$ and the upper set at $z = 1$). The Abaqus mesh seed was set to 1 cm and the element type was set to quadratic hexahedra. The plan view of the resulting region appears in Figure 2. The black edges show the actual curved geometry and the blue edges show what will often be displayed in post-processing applications: linear approximations to the curved edges. Also shown are two encapsulating CSG spheres. The inner sphere (radius of 3 cm) defined the UM universe outer boundary. The outer sphere (radius of 4 cm) defined the extent of the problem, where particles were killed that exit it. All materials were set to void. The black vertices in Figure 2 are at the end of edges and the red vertices are mid-edge and used to define the

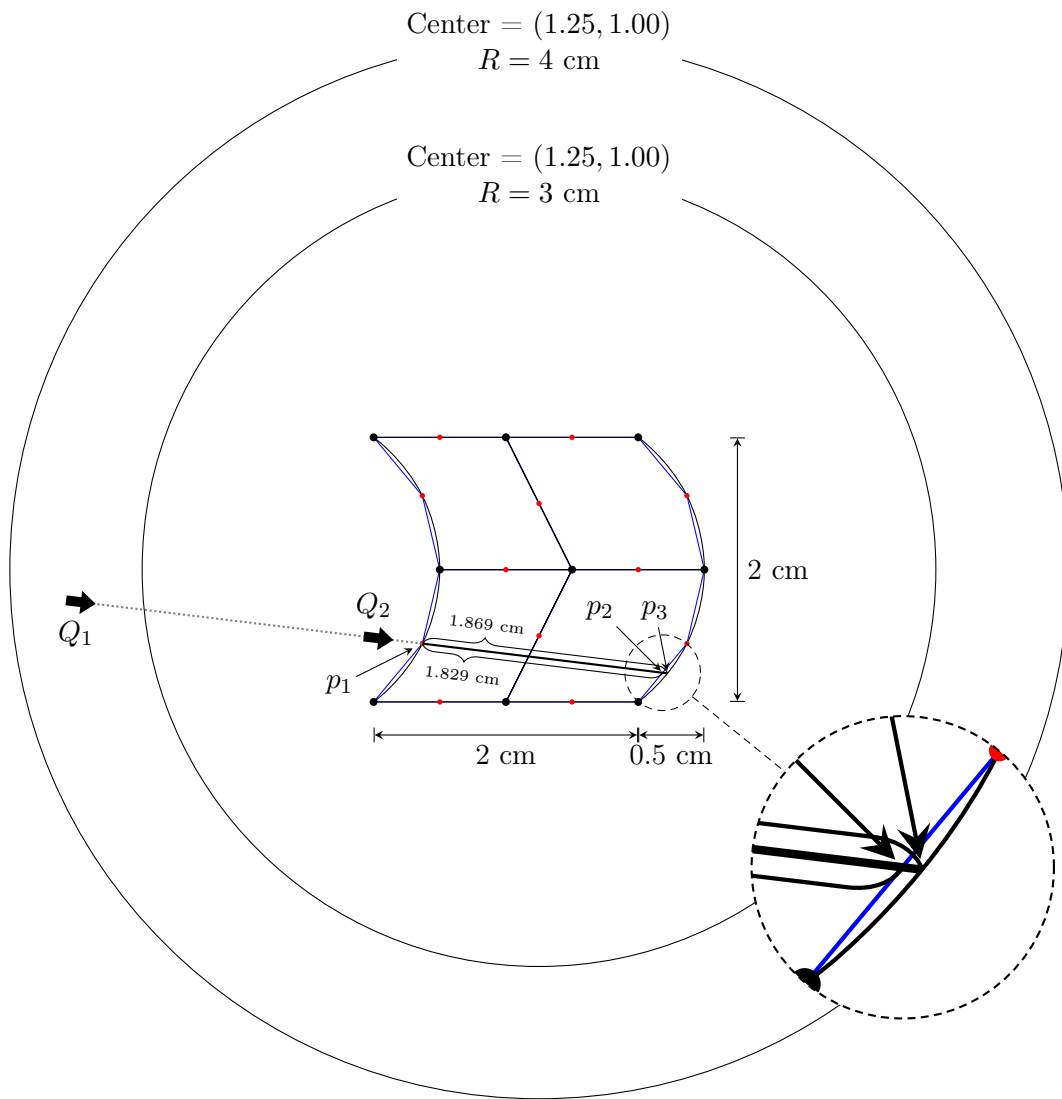


Figure 2: Simple Test Case UM Geometry, Fixed Source Configuration, and Particle Flight Path

curvature of the edge.

The mid-edge vertex at $p_1 = (0.368033975, 0.440982997)$ was used as the point of entry for particles started external to the region. This point was generated by Abaqus as a mid-edge node and it is guaranteed that the edge will pass through it. Thus, it provides an invariant basis to calculate the track length through the UM. The particles were directed from this point toward the point half-way between the lower-right two vertices, $p_2 = (2.18402, 0.220491)$.

If the element would have been flat, the calculated track length would have been calculated to be 1.82932 cm. To find the track length for the curved face, the intersection point of a line representing the particle path and the circular arc representing the curved surface had to be found. The line representing the particle path passes through p_1 and p_2 , and was $y = -0.121417x + 0.485669$. The convex boundary was a circular arc corresponding to a circle centered at $(1.25, 1)$ with radius 1.25 cm. The intersection point of interest for the line and circle was $p_3 = (2.22334, 0.215716)$ so the track length with second-order curvature was 1.86894 cm. This was the value expected for the total track length through the UM.

Two source points were used, with one outside the UM universe and one inside. The outside point, Q_1 , was positioned at $(x, y, z) = (-2.25, 0.758857, 0.5)$ and the inside point, Q_2 , was positioned at $(x, y, z) = (0, 0.485669, 0.5)$. Both sources were given an initial direction of $(u, v, w) = (1, -0.121417, 0)$. Two source points were used to show that correct tracking was performed regardless of whether the source was inside or outside the UM universe.

2.3 Test System

All benchmark problems were run on a Dell Precision Tower 5810 with an Intel Xeon (4 core) E5-1607 v3 chip running at 3.10 GHz. Total cache size was 10,240 kB. Total available RAM was 16,388,196 kB. The operating system was Redhat 6. The simple geometry problem was run on a Late 2013 Mac Pro with the OS X 10.11.6 operating system.

3 Results

3.1 Comparison Objective

The work discussed in this report achieves two objectives:

1. verify that UM models using second-order elements produce acceptable results when compared to models that use MCNP's legacy constructive solid geometry (CSG) capability and/or compared to experimental results, and
2. better understand the performance aspects of UM models that use second-order elements.

3.2 Criticality Results

All of the criticality benchmark problems were run with several different levels of mesh refinement and both first- and second-order elements to see how these parameters affected K_{eff} results and code performance.

Currently, the only way (for LANL) to produce UM models with second-order elements is to create the mesh in Abaqus/CAE [9]. As one of the inputs to the Abaqus meshing tool, a "seed" value is required. This seed is the maximum edge length for any edge of any element. The seed value dictates the number of elements in any part with a larger seed producing a smaller

number of elements. In the tables that follow, the seed value and the corresponding number of elements that is produced differentiate the cases completed in this work.

Each set of calculations was completed with the MCNP6 version (called here 6.2.1) that includes the improved second-order element tracking routines and with the MCNP6 version (called here 6.1.4) that has the older second-order element tracking routines consistent with the 6.1.1 and 6.2.0 version releases to RSICC.

Other data that appear in the criticality results tables are as follows:

1. Mass in grams as calculated by MCNP6. The values are taken from print tables 50 and 60.
2. Mass ratio is the mass from the UM model divided by the mass of the simple sphere in the CSG model. For the Godiva problems, there is only 1 region and 1 mass ratio. For the Big Ten problems, there are 2 regions and 2 mass ratios—one for the enriched uranium region and one for the depleted uranium region.
3. K_{eff} is the eigenvalue calculated by MCNP6. The number in parentheses is the absolute, one-sigma uncertainty of the last two decimal places.
4. ΔK_{eff} is the difference between the CSG (simple) and UM case (with CSG taken as the reference) given in pcm (*percent mille*).
5. K_{eff} ratio is the quotient of K_{eff} in the UM case divided by the K_{eff} of the reference case (simple sphere, CSG model).
6. M Hist / Hr is MCNP6's rate of processing particle histories expressed in millions of histories per hour. The time used in this metric is the wall clock time from the calculation.
7. M Hist Ratio is the quotient of the reference case (simple sphere, CSG model) M Hist / Hr divided by the case M Hist / Hr. This is a measure of how much slower the UM model is compared to the simple sphere model.
8. Memory is the amount of estimated permanent memory needed by MCNP6 for the UM feature. Permanent memory refers to the amount of RAM needed by the code for the UM feature during the calculation and does not include estimated memory for input processing. An estimate of UM memory usage appears in the MCNP6 outp file.
9. Memory / Element is the amount of permanent, UM memory needed by MCNP6 when amortized over the total number of elements in the UM model.

3.2.1 Godiva Results

All of the Godiva problems were run for a total of 2000 cycles with 5000 histories per cycle. The number of skipped cycles in each case was 100.

Tables 1–7 provide results and performance data from the Godiva criticality calculations. Tables 1, 3, and 5 provide the K_{eff} results for the tetrahedral, pentahedral, and hexahedral models, respectively. Tables 2, 4, and 6 provide the performance results for the tetrahedral, pentahedral, and hexahedral models, respectively. Table 7 provides some expanded results that are used to compare the effectiveness of the first and second order tetrahedra.

Calculational Results An examination of the mass results from Tables 1, 3, and 5 shows that the second-order elements did a good job of preserving the correct mass in almost all cases. The worst cases for second-order elements were the coarsest meshes for the pentahedra (seeds of 3.0 and 4.0) and the hexahedra (seed of 5.0). For these three cases, the maximum mass deficiency was approximately 0.4%. In contrast, most of the finely-resolved, first-order models had difficulty preserving the mass with a deficiency of less than 0.4%; the first-order, coarse meshes were worse. This information shows that second-order elements can reduce the mesh count by roughly a factor of 100 (or slightly more) and still preserve the mass.

The impact of the mass deficiency can be seen with the K_{eff} results. With the new, second-order, tracking treatment, 10 of the 21 cases (run with version 6.2.1) were within one standard deviation (1-sigma) of the reference case (simple sphere, CSG model) eigenvalue, 5 were within 2-sigma, and 3 were within 3-sigma. The three cases with the largest mass differences disagreed by more than 3-sigma. The old, second order, tracking treatment (run with version 6.1.4) did not agree as well: there were more cases that agreed only at a 3-sigma level. None of the first-order cases, run with 6.2.1 or 6.1.4, were in agreement within 5-sigma.

Performance Results Tables 2, 4, and 6 reveal some interesting performance insights regarding memory usage and processing speed.

The memory usage shows that specifying second-order elements does require more memory, but the increase is not dramatic. The UM memory can be broken into two large categories: element direct and element indirect. The element-direct category increases every time an element is added to the mesh because memory is needed to store node locations, node connectivity information, etc. The indirect category is needed to store data such as cell, material, edit, etc. information. From the Memory / Element columns in the tables, the effect of amortizing the indirect memory over all elements can be seen. From the Memory / Element numbers it can be seen that the memory cost of using second-order tetrahedra in place of first-order tetrahedra is approximately 3% more. When the same comparison is made for pentahedra and hexahedra, it can be seen that the additional memory costs are approximately 18% and 24%, respectively.

In lieu of what was stated above with respect to needing fewer second-order elements to accurately model the system, it may be more advantageous to use second-order elements if the model is so large that total memory usage is an issue. Cutting the element count by a factor of 100 easily compensates for an increase of 24% in memory to use second-order hexahedra in place of first-order ones. These statements concerning memory are independent of the code version.

The processing speed results in Tables 2, 4, and 6 show more interesting behavior. There is no doubt from these tables that tracking with first-order elements is faster provided the number of elements is held constant. Interestingly, the refactored top-level tracking loop [10] of version 6.2.1 is a few percent faster than the 6.1.4 version.

The most dramatic performance result that the tables reveal is the speed improvement for all second-order elements with the 6.2.1 version compared to the 6.1.4 version. For the coarse element models, the speed increase is approximately a factor of 3.7, depending upon element type. For the more detailed element models, the speed increase is as high as 4 to 5.2.

Another way of viewing the second-order processing time improvement is to compare the processing times to the corresponding first-order element processing times. From the 6.1.4 version results, the second-order calculations were anywhere from a factor of 10 to factor of 19 slower. From the 6.2.1 version results, the second-order calculations were anywhere from a factor of 2.1 to 5.5 slower, depending upon element type. These values aren't explicitly provided

in the tables.

A casual comparison of 6.2.1 processing times by element type appears to show that the preferred order (i.e., which are most efficient) for using elements are tetrahedra, pentahedra, and hexahedra. However, if the M Hist / Hr results are normalized by the number of elements in the model, then the order is reversed to be hexahedra, pentahedra, and tetrahedra. For the most finely resolved models in the table, the M Hist / Hr / Element numbers are 0.00029 (tets), 0.00102 (pents), and 0.00215 (hexs).

Comparison of First and Second Order Tetrahedra For a fixed number of elements, tracking on first-order elements has been shown to be faster than tracking on second-order elements. Second-order elements have been shown to more accurately model parts with curved surfaces, hence preserving volume and mass. Correspondingly, fewer second-order elements are needed to preserve volumes and masses to within a pre-selected tolerance. One might ask: which type of elements is more effective? Here, effective is taken to mean “producing the more/most accurate results in the least amount of time.”

To address the issue of effectiveness, the set of first-order tetrahedral models for the Godiva problem was expanded. Several more finely-meshed, first-order tetrahedral models were created and run to see how the accuracy of the calculated K_{eff} and timing changed. These additional results are provided in Table 7 along with the previous first- and second-order tetrahedral results from Tables 1 and 2.

More than tripling the number of first-order tetrahedra (seed 0.5; 145156 elements) over what was previously the finest (seed 0.8; 45756 elements) first-order tetrahedra resolution did not substantially improve the Mass Ratio and the resulting K_{eff} was still greater than 3-sigma from the reference value. Even a 5.8 \times increase in the number of tetrahedra (seed 0.4; 265931 elements) had little effect on improving preservation of the critical mass. The M Hist / Hr value of 19.35 was 50% slower than the 29.10 M Hist / Hr value obtained with the coarser-meshed second-order element case (seed 3.0; 1281 elements) that was able to match the K_{eff} to well within 1-sigma

For a fixed number of elements, first-order elements are faster. However, this work shows that when accuracy is desired (particularly when using curved parts) not only can second-order elements preserve the mass with fewer elements, it can produce the answer more quickly.

Table 1: Godiva Tetrahedron Results Comparison

Element Type	Seed (cm)	Elements	Mass (gm)	Mass Ratio	K_{eff}	ΔK_{eff} (pcm)	K_{eff} Ratio
2nd Order / 6.2.1	0.8	45756	5.24253E+04	1.00000	1.00114(19)	-20.0	0.99980
	1.0	24013	5.24251E+04	1.00000	1.00105(19)	-29.0	0.99971
	1.2	13854	5.24248E+04	0.99999	1.00149(20)	15.0	1.00015
	1.5	7527	5.24241E+04	0.99997	1.00147(19)	13.0	1.00013
	3.0	1281	5.24151E+04	0.99980	1.00143(19)	9.0	1.00009
	5.0	271	5.23679E+04	0.99890	1.00129(20)	-5.0	0.99995
1st Order / 6.2.1	0.8	45756	5.22244E+04	0.99617	1.00032(20)	-102.0	0.99898
	1.0	24013	5.20976E+04	0.99375	0.99904(19)	-230.0	0.99770
	1.2	13854	5.19278E+04	0.99051	0.99895(20)	-239.0	0.99761
	1.5	7527	5.16873E+04	0.98592	0.99715(19)	-419.0	0.99582
	3.0	1281	5.03177E+04	0.95980	0.98956(19)	-1178.0	0.98824
	5.0	271	4.75219E+04	0.90647	0.97302(19)	-2832.0	0.97172
2nd Order / 6.1.4	0.8	45756	5.24253E+04	1.00000	1.00144(20)	10.0	1.00010
	1.0	24013	5.24251E+04	1.00000	1.00120(19)	-14.0	0.99986
	1.2	13854	5.24248E+04	0.99999	1.00145(20)	11.0	1.00011
	1.5	7527	5.24241E+04	0.99997	1.00051(20)	-83.0	0.99917
	3.0	1281	5.24151E+04	0.99980	1.00079(19)	-55.0	0.99945
	5.0	271	5.23679E+04	0.99890	1.00095(19)	-39.0	0.99961
1st Order / 6.1.4	0.8	45756	5.22244e+04	0.99617	1.00032(20)	-102.0	0.99898
	1.0	24013	5.20976E+04	0.99375	0.99904(19)	-230.0	0.99770
	1.2	13854	5.19278E+04	0.99051	0.99895(20)	-239.0	0.99761
	1.5	7527	5.16873E+04	0.98592	0.99715(19)	-419.0	0.99582
	3.0	1281	5.03177E+04	0.95980	0.98956(19)	-1178.0	0.98824
	5.0	271	4.75219E+04	0.90647	0.97302(19)	-2832.0	0.97172
CSG			5.24254e+04	1.0	1.00134(20)	0.0	1.00000

Table 2: Godiva Tetrahedron Performance Comparison

Element Type	Seed (cm)	Number Of Elements	M Hist / Hr	M Hist Ratio	Memory (bytes)	Memory / Element (bytes)
2nd Order / 6.2.1	0.8	45756	13.30	19.78	21503778	470
	1.0	24013	16.34	16.10	11337896	472
	1.2	13854	18.80	14.00	6569894	474
	1.5	7527	21.66	12.15	3598252	478
	3.0	1281	29.10	9.04	610498	477
	5.0	271	32.62	8.07	165700	611
1st Order / 6.2.1	0.8	45756	28.08	9.37	20896794	457
	1.0	24013	36.00	7.31	11013480	459
	1.2	13854	41.62	6.32	6379550	460
	1.5	7527	48.77	5.40	3491692	464
	3.0	1281	72.60	3.62	590170	485
	5.0	271	96.07	2.74	159764	590
2nd Order / 6.1.4	0.8	45756	2.66	98.92	21503778	470
	1.0	24013	3.23	81.47	11337896	472
	1.2	13854	3.73	70.55	6569894	474
	1.5	7527	4.40	59.80	3598252	478
	3.0	1281	6.64	39.63	610498	477
	5.0	271	8.51	30.92	165700	611
1st Order / 6.1.4	0.8	45756	26.99	9.75	20896794	457
	1.0	24013	33.56	7.84	11013480	459
	1.2	13854	39.08	6.73	6379550	460
	1.5	7527	45.40	5.80	3491692	464
	3.0	1281	68.26	3.85	590170	485
	5.0	271	89.35	2.95	159764	590
CSG			263.14	1.0		

Table 3: Godiva Pentahedron Results Comparison

Element Type	Seed (cm)	Elements	Mass (gm)	Mass Ratio	K_{eff}	ΔK_{eff} (pcm)	K_{eff} Ratio
2nd Order / 6.2.1	0.8	13120	5.24250E+04	0.99999	1.00110(20)	-24.0	0.99976
	1.0	6400	5.24247E+04	0.99999	1.00132(19)	-2.0	0.99998
	1.2	3096	5.24233E+04	0.99996	1.00125(20)	-9.0	0.99991
	1.5	1248	5.24166E+04	0.99983	1.00103(20)	-31.0	0.99969
	2.0	596	5.24038E+04	0.99959	1.00085(19)	-49.0	0.99951
	3.0	176	5.22880E+04	0.99738	0.99902(19)	-231.0	0.99769
	4.0	80	5.21651E+04	0.99503	0.99760(19)	-374.0	0.99627
1st Order / 6.2.1	0.8	13120	5.21000E+04	0.99379	1.00007(19)	-127.0	0.99873
	1.0	6400	5.19447E+04	0.99083	0.99819(20)	-315.0	0.99685
	1.2	3096	5.15928E+04	0.98412	0.99681(19)	-453.0	0.99548
	1.5	1248	5.06706E+04	0.96653	0.99169(19)	-965.0	0.99036
	2.0	596	4.97130E+04	0.94826	0.98617(19)	-1517.0	0.98485
	3.0	176	4.57659E+04	0.87297	0.96214(19)	-3920.0	0.96085
	4.0	80	4.39749E+04	0.83881	0.95151(19)	-4983.0	0.95024
2nd Order / 6.1.4	0.8	13120	5.24250E+04	0.99999	1.00144(20)	10.0	1.00010
	1.0	6400	5.24247E+04	0.99999	1.00151(19)	17.0	1.00017
	1.2	3096	5.24233E+04	0.99996	1.00110(20)	-24.0	0.99976
	1.5	1248	5.24166E+04	0.99983	1.00107(20)	-27.0	0.99973
	2.0	596	5.24038E+04	0.99959	1.00085(19)	-49.0	0.99951
	3.0	176	5.22880E+04	0.99738	0.99973(20)	-161.0	0.99839
	4.0	80	5.21651E+04	0.99503	0.99874(20)	-260.0	0.99740
1st Order / 6.1.4	0.8	13120	5.21000E+04	0.99379	1.00007(19)	-127.0	0.99873
	1.0	6400	5.19447E+04	0.99083	0.99819(20)	-315.0	0.99685
	1.2	3096	5.15928E+04	0.98412	0.99681(19)	-453.0	0.99548
	1.5	1248	5.06706E+04	0.96653	0.99169(19)	-965.0	0.99036
	2.0	596	4.97130E+04	0.94826	0.98617(19)	-1517.0	0.98485
	3.0	176	4.57659E+04	0.87297	0.96214(19)	-3920.0	0.96085
	4.0	80	4.39749E+04	0.83881	0.95151(19)	-4983.0	0.95024
CSG			5.24254e+04	1.0	1.00134(20)	0.0	1.00000

Table 4: Godiva Pentahedron Performance Comparison

Element Type	Seed (cm)	Number Of Elements	M Hist / Hr	M Hist Ratio	Memory (bytes)	Memory / Element (bytes)
2nd Order / 6.2.1	0.8	13120	13.33	19.74	7485614	571
	1.0	6400	15.33	17.17	3689462	576
	1.2	3096	17.89	14.71	1807654	584
	1.5	1248	20.36	12.92	739022	592
	2.0	596	21.64	12.16	372206	625
	3.0	176	24.48	10.75	131726	748
	4.0	80	25.83	10.19	75502	944
1st Order / 6.2.1	0.8	13120	39.21	6.71	6349742	484
	1.0	6400	47.50	5.54	3130358	489
	1.2	3096	56.38	4.67	1534270	496
	1.5	1248	68.84	3.82	627422	503
	2.0	596	77.59	3.39	317630	533
	3.0	176	98.04	2.68	114974	653
	4.0	80	108.11	2.43	67534	844
2nd Order / 6.1.4	0.8	13120	2.55	103.19	7485614	571
	1.0	6400	3.09	85.16	3689462	576
	1.2	3096	3.59	75.30	1807654	584
	1.5	1248	4.32	60.91	739022	592
	2.0	596	4.90	53.70	372206	625
	3.0	176	6.05	43.39	131726	748
	4.0	80	6.82	38.58	75502	944
1st Order / 6.1.4	0.8	13120	39.03	6.74	6349742	484
	1.0	6400	46.09	5.71	3130358	489
	1.2	3096	53.81	4.89	1534270	496
	1.5	1248	65.44	4.02	627422	503
	2.0	596	73.61	3.57	317630	533
	3.0	176	92.52	2.84	114974	653
	4.0	80	103.38	2.55	67534	844
CSG			263.14	1.0		

Table 5: Godiva Hexahedron Results Comparison

Element Type	Seed (cm)	Elements	Mass (gm)	Mass Ratio	K_{eff}	ΔK_{eff} (pcm)	K_{eff} Ratio
2nd Order / 6.2.1	1.0	5096	5.24251E+04	1.00000	1.00143(19)	9.0	1.00009
	1.2	2880	5.24246E+04	0.99999	1.00111(19)	-23.0	0.99977
	1.5	1320	5.24237E+04	0.99997	1.00123(20)	-11.0	0.99989
	1.7	896	5.24222E+04	0.99994	1.00147(20)	13.0	1.00013
	2.0	552	5.24185E+04	0.99987	1.00106(20)	-28.0	0.99972
	3.0	224	5.23951E+04	0.99942	1.00087(19)	-47.0	0.99953
	4.0	160	5.23710E+04	0.99896	1.00089(20)	-45.0	0.99955
	5.0	56	5.21104E+04	0.99399	0.99951(19)	-183.0	0.99817
1st Order / 6.2.1	1.0	5096	5.21360E+04	0.99448	1.00019(19)	-115.0	0.99885
	1.2	2880	5.19765E+04	0.99144	0.99896(20)	-238.0	0.99762
	1.5	1320	5.17584E+04	0.98728	0.99748(19)	-386.0	0.99615
	1.7	896	5.15365E+04	0.98305	0.99656(19)	-478.0	0.99523
	2.0	552	5.11128E+04	0.97496	0.99428(19)	-706.0	0.99295
	3.0	224	4.97335E+04	0.94865	0.98659(19)	-1475.0	0.98527
	4.0	160	4.89155E+04	0.93305	0.98159(20)	-1975.0	0.98028
	5.0	56	4.40454E+04	0.84015	0.95216(19)	-4918.0	0.95089
2nd Order / 6.1.4	1.0	5096	5.24251E+04	1.00000	1.00128(20)	-6.0	0.99994
	1.2	2880	5.24246E+04	0.99999	1.00110(19)	-24.0	0.99976
	1.5	1320	5.24237E+04	0.99997	1.00087(19)	-47.0	0.99953
	1.7	896	5.24222E+04	0.99994	1.00101(20)	-33.0	0.99967
	2.0	552	5.24185E+04	0.99987	1.00114(19)	-20.0	0.99980
	3.0	224	5.23951E+04	0.99942	1.00129(20)	-5.0	0.99995
	4.0	160	5.23710E+04	0.99896	1.00128(19)	-6.0	0.99994
	5.0	56	5.21104E+04	0.99399	0.99971(19)	-163.0	0.99837
1st Order / 6.1.4	1.0	5096	5.21360E+04	0.99448	1.00019(19)	-115.0	0.99885
	1.2	2880	5.19765E+04	0.99144	0.99896(20)	-238.0	0.99762
	1.5	1320	5.17584E+04	0.98728	0.99748(19)	-386.0	0.99615
	1.7	896	5.15365E+04	0.98305	0.99656(19)	-478.0	0.99523
	2.0	552	5.11128E+04	0.97496	0.99428(19)	-706.0	0.99295
	3.0	224	4.97335E+04	0.94865	0.98659(19)	-1475.0	0.98527
	4.0	160	4.89155E+04	0.93305	0.98159(20)	-1975.0	0.98028
	5.0	56	4.40454E+04	0.84015	0.95216(19)	-4918.0	0.95089
CSG			5.24254e+04	1.0	1.00134(20)	0.0	1.00000

Table 6: Godiva Hexahedron Performance Comparison

Element Type	Seed (cm)	Number Of Elements	M Hist / Hr	M Hist Ratio	Memory (bytes)	Memory / Element (bytes)
2nd Order / 6.2.1	1.0	5096	10.96	24.01	3325294	653
	1.2	2880	13.43	19.59	1488878	517
	1.5	1320	14.74	17.85	901774	683
	1.7	986	15.85	16.60	620686	693
	2.0	552	17.16	15.33	397070	719
	3.0	224	19.07	13.80	179822	803
	4.0	160	19.91	13.22	136398	852
	5.0	56	19.81	13.28	65070	1162
1st Order / 6.2.1	1.0	5096	50.58	5.20	2684446	527
	1.2	2880	61.41	4.28	1204622	418
	1.5	1320	67.97	3.87	730174	553
	1.7	986	73.12	3.60	503326	562
	2.0	552	79.25	3.32	323966	587
	3.0	224	91.86	2.86	149486	667
	4.0	160	95.86	2.75	114558	716
	5.0	56	109.90	2.39	57150	1021
2nd Order / 6.1.4	1.0	5096	2.74	96.04	3325294	653
	1.2	2880	3.34	78.78	1488878	517
	1.5	1320	3.72	70.74	901774	683
	1.7	986	4.00	65.79	620686	693
	2.0	552	4.33	60.77	397070	719
	3.0	224	4.87	54.03	179822	803
	4.0	160	5.08	51.80	136398	852
	5.0	56	5.51	47.76	65070	1162
1st Order / 6.1.4	1.0	5096	48.14	5.47	2684446	527
	1.2	2880	58.42	4.50	1204622	418
	1.5	1320	64.79	4.06	730174	553
	1.7	986	70.00	3.76	503326	562
	2.0	552	75.51	3.48	323966	587
	3.0	224	86.89	3.03	149486	667
	4.0	160	90.58	2.91	114558	716
	5.0	56	103.83	2.53	57150	1021
CSG			263.14	1.0		

Table 7: Expanded Godiva Tetrahedron Results

Element Type	Seed (cm)	Elements	Mass (gm)	Mass Ratio	K_{eff}	ΔK_{eff} (pcm)	K_{eff} Ratio	M Hist / Hr
2nd Order / 6.2.1	0.8	45756	5.24253E+04	1.00000	1.00114(19)	-20.0	0.99980	13.30
	1.0	24013	5.24251E+04	1.00000	1.00105(19)	-29.0	0.99971	16.34
	1.2	13854	5.24248E+04	0.99999	1.00149(20)	15.0	1.00015	18.80
	1.5	7527	5.24241E+04	0.99997	1.00147(19)	13.0	1.00013	21.66
	3.0	1281	5.24151E+04	0.99980	1.00143(19)	9.0	1.00009	29.10
	5.0	271	5.23679E+04	0.99890	1.00129(20)	-5.0	0.99995	32.62
1st Order / 6.2.1	0.4	265931	2.79370E+04	0.99913	1.00047(20)	-87.0	0.99913	15.92
	0.45	197201	5.23373E+04	0.99832	1.00091(20)	-43.0	0.99957	17.62
	0.5	145156	5.23069E+04	0.99774	1.00042(19)	-92.0	0.99908	19.35
	0.6	90950	5.22629E+04	0.99690	1.00020(19)	-114.0	0.99886	22.60
	0.8	45756	5.22244E+04	0.99617	1.00032(20)	-102.0	0.99898	28.08
	1.0	24013	5.20976E+04	0.99375	0.99904(19)	-230.0	0.99770	36.00
	1.2	13854	5.19278E+04	0.99051	0.99895(20)	-239.0	0.99761	41.62
	1.5	7527	5.16873E+04	0.98592	0.99715(19)	-419.0	0.99582	48.77
	3.0	1281	5.03177E+04	0.95980	0.98956(19)	-1178.0	0.98824	72.60
	5.0	271	4.75219E+04	0.90647	0.97302(19)	-2832.0	0.97172	96.07

3.2.2 Big Ten Results

All of the Big Ten problems were run for a total of 250 cycles with 20000 histories per cycle. The number of skipped cycles in each case was 30.

Tables 8–13 provide results and performance data from the Big Ten criticality calculations. Tables 8, 10, and 12 provide the K_{eff} results for the tetrahedral, pentahedral, and hexahedral models, respectively. Tables 9, 11, and 13 provide the performance results for the tetrahedral, pentahedral, and hexahedral models, respectively.

Calculational Results An examination of the mass results from Tables 8, 10, and 12 shows that the second-order elements did a good job of preserving the correct mass in all cases.

K_{eff} results were also quite good. With the new, second-order, tracking treatment, 7 of the 12 cases (run with version 6.2.1) were within one standard deviation (1-sigma) of the reference case (simple, CSG model) eigenvalue, 2 were within 2-sigma, and 3 were within 3-sigma. No cases disagreed by more than 3-sigma. As with the Godiva calculations, the old, second-order, tracking treatment (run with version 6.1.4) did not fare quite as well because there were only 3 cases that agreed at the 1-sigma level and agreement for three cases was beyond the 3-sigma level. Only two of the first-order cases, run with 6.2.1 or 6.1.4, were in agreement at the 1-sigma level; the rest agreed beyond 3-sigma.

Performance Results An examination of Tables 9, 11, and 13 reveals some interesting performance insights regarding memory usage and processing speed.

Memory usage for the Big Ten problems was similar to that of the Godiva problems. That memory usage discussion won't be repeated here except to say that for the Big Ten problems the additional memory costs are approximately 3%, 15% and 20% for the tetrahedra, pentahedra, and hexahedra, respectively.

Tables 9, 11, and 13 once again show that tracking with first-order elements is faster than tracking with second-order elements provided the number of elements is held constant. For the pentahedral and hexahedral cases, the refactored top-level tracking loop [10] of version 6.2.1 is a few percent faster than the 6.1.4 version for the first order elements. For the first-order tetrahedra, two cases were slower (1 to 9%) and two cases were faster (12 to 26%).

The most dramatic performance result that the tables reveal was the speed improvement for all second-order elements with the 6.2.1 version compared to the 6.1.4 version. Because the variability in the number of elements was not as great in the Big Ten models as compared to the Godiva models, the spread in the speed increase was a little smaller. The speed increases were in the range of 3.9 to 4.9 (consistent with what was seen with the Godiva calculations).

Comparing the second-order history-processing times to the corresponding first-order element processing times shows similar behavior as to what was seen with the Godiva calculations. From the 6.1.4 version results, the second-order calculations were anywhere from a factor of 8.2–17.6 slower. From the 6.2.1 version results, the second-order calculations were anywhere from a factor of 2.4 to 4.2 slower, depending upon element type.

Big Ten results based on the M Hist / Hour / Element metric show that the preferred order for using the elements is hexahedra, pentahedra, and tetrahedra, as was the case for the Godiva calculations.

Table 8: Big Ten Tetrahedron Results Comparison

Element Type	Seed (cm)	Elements	Mass #1 (gm)	Mass #2 (gm)	Mass Ratio #1	Mass Ratio #2	K _{eff}	ΔK _{eff} (pcm)	K _{eff} Ratio
2nd Order / 6.2.1	7	11650	2.44364E+6	7.62664E+6	0.99999	1.00000	0.99468(23)	-2.0	0.99998
	8	7503	2.44361E+6	7.62665E+6	0.99998	1.00000	0.99500(25)	30.0	1.00030
	10	4732	2.44354E+6	7.62670E+6	0.99995	1.00001	0.99544(23)	74.0	1.00074
	12	2509	2.44361E+6	7.62648E+6	0.99998	0.99998	0.99484(25)	14.0	1.00014
1st Order / 6.2.1	7	11650	2.41584E+6	7.60333E+6	0.98862	0.99695	0.99322(26)	-148.0	0.99851
	8	7503	2.40366E+6	7.60194E+6	0.98363	0.99676	0.99308(21)	-162.0	0.99837
	10	4732	2.38134E+6	7.60446E+6	0.97450	0.99709	0.99161(24)	-309.0	0.99689
	12	2509	2.38134E+6	7.57416E+6	0.97450	0.99312	0.99253(26)	-217.0	0.99782
2nd Order / 6.1.4	7	11650	2.44364E+6	7.62664E+6	0.99999	1.00000	0.99428(25)	-42.0	0.99958
	8	7503	2.44361E+6	7.62665E+6	0.99998	1.00000	0.99452(24)	-18.0	0.99982
	10	4732	2.44354E+6	7.62670E+6	0.99995	1.00001	0.99346(25)	-124.0	0.99875
	12	2509	2.44361E+6	7.62648E+06	0.99998	0.99998	0.99379(25)	-91.0	0.99909
1st Order / 6.1.4	7	11650	2.41584E+6	7.60333E+6	0.98862	0.99695	0.99322(26)	-148.0	0.99851
	8	7503	2.40366E+6	7.60194E+6	0.98363	0.99676	0.99308(21)	-162.0	0.99837
	10	4732	2.38134E+6	7.60446E+6	0.97450	0.99709	0.99161(24)	-309.0	0.99689
	12	2509	2.38134E+6	7.57416E+6	0.97450	0.99312	0.99253(26)	-217.0	0.99782
CSG			2.44366E+6	7.62663E+6	1.0	1.0	0.99470(24)	0.0	1.00000

Table 9: Big Ten Tetrahedron Performance Comparison

Element Type	Seed (cm)	Number Of Elements	M Hist / Hr	M Hist Ratio	Memory (bytes)	Memory / Element (bytes)
2nd Order / 6.2.1	7	11650	4.50	6.54	5952496	511
	8	7503	4.66	6.32	3877722	517
	10	4732	4.81	6.12	2465756	521
	12	2509	4.79	6.14	1335926	532
1st Order / 6.2.1	7	11650	10.66	2.76	5785544	497
	8	7503	11.12	2.65	3767274	502
	10	4732	11.91	2.47	2394108	506
	12	2509	12.55	2.35	1332616	531
2nd Order / 6.1.4	7	11650	1.03	28.57	5952496	511
	8	7503	1.09	27.00	3877722	517
	10	4732	1.15	25.59	2465756	521
	12	2509	1.22	24.12	1335926	532
1st Order / 6.1.4	7	11650	11.73	2.51	5785544	497
	8	7503	11.20	2.63	3767274	502
	10	4732	10.63	2.77	2394108	506
	12	2509	9.99	2.95	1332616	531
CSG			29.43			

Table 10: Big Ten Pentahedron Results Comparison

Element Type	Seed (cm)	Elements	Mass #1 (gm)	Mass #2 (gm)	Mass Ratio #1	Mass Ratio #2	Mass Ratio #2	K_{eff}	ΔK_{eff} (pcm)	K_{eff} Ratio
2nd Order / 6.2.1	7	3682	2.44364E+6	7.62663E+6	0.99999	1.00000	0.99545(26)	75.0	1.00075	
	8	2436	2.44362E+6	7.62664E+6	0.99998	1.00000	0.99489(22)	19.0	1.00019	
	10	1630	2.44357E+6	7.62666E+6	0.99996	1.00000	0.99482(23)	12.0	1.00012	
	12	776	2.44349E+6	7.62667E+6	0.99994	1.00001	0.99494(23)	24.0	1.00024	
1st Order / 6.2.1	7	3682	2.41888E+6	7.59693E+6	0.98986	0.99611	0.99353(23)	-117.0	0.99882	
	8	2436	2.40855E+6	7.59215E+6	0.98564	0.99548	0.99305(25)	-165.0	0.99834	
	10	1630	2.38996E+6	7.58830E+6	0.97803	0.99498	0.99188(26)	-282.0	0.99716	
	12	776	2.37497E+6	7.56797E+6	0.97189	0.99231	0.99120(22)	-350.0	0.99648	
2nd Order / 6.1.4	7	3682	2.44364E+6	7.62663E+6	0.99999	1.00000	0.99453(24)	-17.0	0.99983	
	8	2436	2.44362E+6	7.62664E+6	0.99998	1.00000	0.99454(24)	-16.0	0.99984	
	10	1630	2.44357E+6	7.62666E+6	0.99996	1.00000	0.99373(23)	-97.0	0.99902	
	12	776	2.44349E+6	7.62667E+6	0.99994	1.00001	0.99400(22)	-70.0	0.99930	
1st Order / 6.1.4	7	3682	2.41888E+6	7.59693E+6	0.98986	0.99611	0.99353(23)	-117.0	0.99882	
	8	2436	2.40855E+6	7.59215E+6	0.98564	0.99548	0.99305(25)	-165.0	0.99834	
	10	1630	2.38996E+6	7.58830E+6	0.97803	0.99498	0.99188(26)	-282.0	0.99716	
	12	776	2.37497E+6	7.56797E+6	0.97189	0.99231	0.99120(22)	-350.0	0.99648	
CSG			2.44366E+6	7.62663E+6	1.0	1.0	0.99470(24)	0.0	1.00000	

Table 11: Big Ten Pentahedron Performance Comparison

Element Type	Seed (cm)	Number Of Elements	M Hist / Hr	M Hist Ratio	Memory (bytes)	Memory / Element (bytes)
2nd Order / 6.2.1	7	3682	4.76	6.18	2400728	652
	8	2436	4.88	6.03	1627840	668
	10	1630	4.98	5.91	1098632	674
	12	776	4.90	6.01	561832	724
1st Order / 6.2.1	7	3682	11.42	2.58	2069456	562
	8	2436	11.82	2.49	1406320	577
	10	1630	12.24	2.40	948800	582
	12	776	12.82	2.30	488272	629
2nd Order / 6.1.4	7	3682	0.98	30.03	2400728	652
	8	2436	1.01	29.14	1627840	668
	10	1630	1.05	28.03	1098632	674
	12	776	1.06	27.76	561832	724
1st Order / 6.1.4	7	3682	10.81	2.72	2069456	562
	8	2436	11.05	2.66	1406320	577
	10	1630	11.45	2.57	948800	582
	12	776	12.09	2.43	488272	629
CSG			29.43			

Table 12: Big Ten Hexahedron Results Comparison

Element Type	Seed (cm)	Elements	Mass #1 (gm)	Mass #2 (gm)	Mass Ratio #1	Mass Ratio #2	Mass Ratio #2	K _{eff}	ΔK _{eff} (pcm)	K _{eff} Ratio
2nd Order / 6.2.1	7	1848	2.44365e+6	7.62659e+6	1.00000	1.00000	0.99461(24)	0.99991	-9.0	0.99991
	8	1248	2.44364e+6	7.62656e+6	0.99999	0.99999	0.99512(23)	1.00042	42.0	1.00042
	10	840	2.44361e+6	7.62648e+6	0.99998	0.99998	0.99516(24)	1.00046	46.0	1.00046
	12	512	2.44361e+6	7.62648e+6	0.99998	0.99998	0.99471(23)	1.00001	1.0	1.00001
1st Order / 6.2.1	7	1848	2.42321e+6	7.56279e+6	0.99163	0.99163	0.99455(25)	0.99985	-15.0	0.99985
	8	1248	2.41584e+6	7.53981e+6	0.98862	0.98862	0.99368(23)	0.99897	-102.0	0.99897
	10	840	2.40366e+6	7.50180e+6	0.98363	0.98363	0.99255(23)	0.99784	-215.0	0.99784
	12	512	2.40366e+6	7.50180e+6	0.98363	0.98363	0.99336(25)	0.99865	-134.0	0.99865
2nd Order / 6.1.4	7	1848	2.44365e+6	7.62659e+6	1.00000	1.00000	0.99437(24)	0.99967	-33.0	0.99967
	8	1248	2.44364e+6	7.62656e+6	0.99999	0.99999	0.99442(23)	0.99972	-28.0	0.99972
	10	840	2.44361e+6	7.62648e+6	0.99998	0.99998	0.99416(24)	0.99946	-54.0	0.99946
	12	512	2.44361e+6	7.62648e+6	0.99998	0.99998	0.99396(24)	0.99926	-74.0	0.99926
1st Order / 6.1.4	7	1848	2.42321e+6	7.56279e+6	0.99163	0.99163	0.99455(25)	0.99985	-15.0	0.99985
	8	1248	2.41584e+6	7.53981e+6	0.98862	0.98862	0.99368(23)	0.99897	-102.0	0.99897
	10	840	2.40366e+6	7.50180e+6	0.98363	0.98363	0.99255(23)	0.99784	-215.0	0.99784
	12	512	2.40366e+6	7.50180e+6	0.98363	0.98363	0.99336(25)	0.99865	-134.0	0.99865
CSG			2.44366E+6	7.62663E+6	1.0	1.0	0.99470(24)	1.00000	0.0	1.00000

Table 13: Big Ten Hexahedron Performance Comparison

Element Type	Seed (cm)	Number Of Elements	M Hist / Hr	M Hist Ratio	Memory (bytes)	Memory / Element (bytes)
2nd Order / 6.2.1	7	1848	2.95	9.98	1395004	755
	8	1248	3.07	9.59	969068	776
	10	840	3.13	9.40	661468	787
	12	512	3.02	9.75	437644	855
1st Order / 6.2.1	7	1848	11.44	2.57	1156828	626
	8	1248	11.80	2.49	806828	646
	10	840	12.32	2.39	551356	656
	12	512	12.61	2.33	368860	720
2nd Order / 6.1.4	7	1848	0.65	45.28	1395004	755
	8	1248	0.66	44.59	969068	776
	10	840	0.67	43.93	661468	787
	12	512	0.68	43.28	437644	855
1st Order / 6.1.4	7	1848	11.00	2.68	1156828	626
	8	1248	11.31	2.60	806828	646
	10	840	11.58	2.54	551356	656
	12	512	11.98	2.46	368860	720
CSG			29.43			

3.3 Pulsed Sphere Results

The calculated pulsed sphere time spectra from this work with the second-order UM models are shown in Figure 3. Included in the plots are the Legacy CSG calculated results and the experimental results from Reference 8. Results from the CSG Detailed and Hybrid calculations [8] were not included for clarity. These calculations were performed in the same manner as described in Section II.H of Reference 8.

For all calculations, the agreement between the experimental and calculated spectra is qualitatively confirmed through visual inspection. Using a χ^2 goodness-of-fit test shows that unnormalized and normalized calculated and experimental spectra agree with p -values greater than 0.999 in all cases which supports a null hypothesis that a given calculated spectrum behaves comparably to the experimental spectrum.

Next, the fractional errors, ϵ , between the calculated and experimental spectra are determined with

$$\epsilon = \frac{\int_0^\infty [f_{\text{Exp.}}(t) - f_{\text{Calc.}}(t)]^2 dt}{\int_0^\infty [f_{\text{Exp.}}(t)]^2 dt} \rightarrow \frac{\sum_t (f_{t,\text{Exp.}} - f_{t,\text{Calc.}})^2}{\sum_t (f_{t,\text{Exp.}})^2} \quad (1)$$

by recognizing that all time bin widths are identical and that there are an equal amount of bins in the calculated and experimental results. These fractional errors relative to experiment are

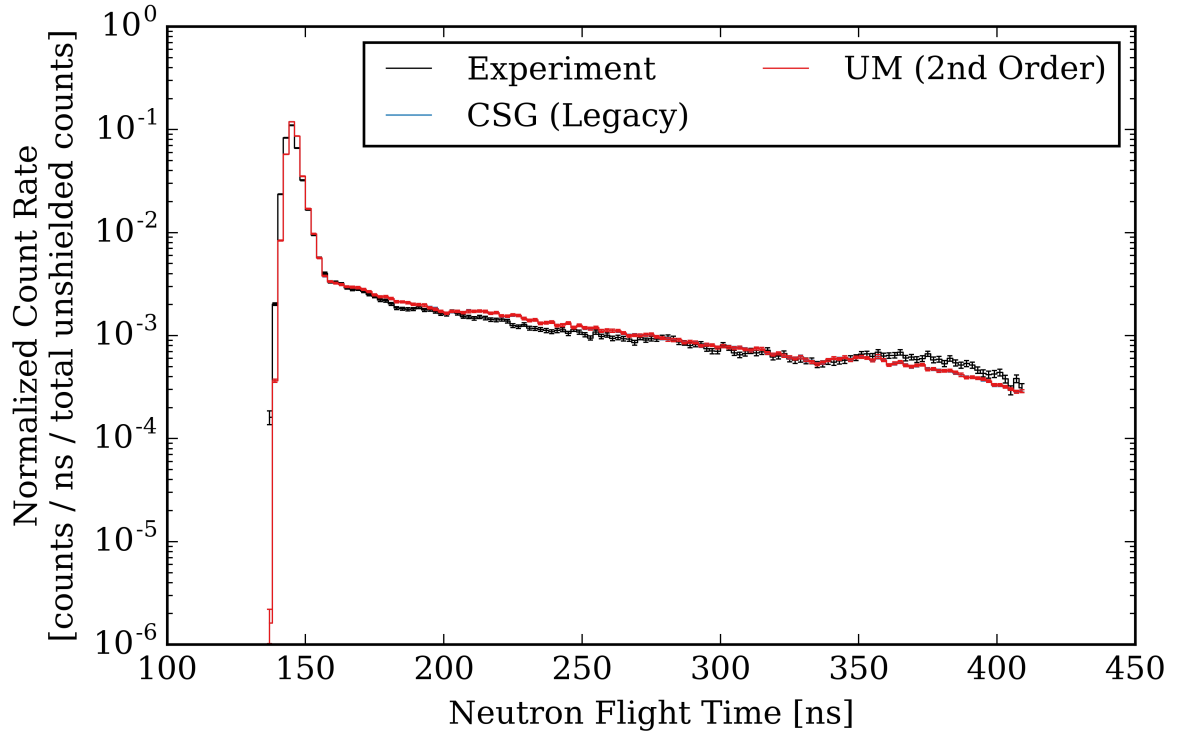
shown in Table 14. It should be recognized that unlike previous work in Reference 11, no points are excluded from either the χ^2 p -value or fractional error calculations. Furthermore, the error observed in the UM models agrees most closely with the Legacy models while the Detailed and Hybrid models behave similarly.

The fractional errors relative to the Legacy calculated spectra are given in Table 15. Agreement is well within 1% for the UM and CSG models. This is not surprising because the maximum mass deviation between the models was 0.00042%.

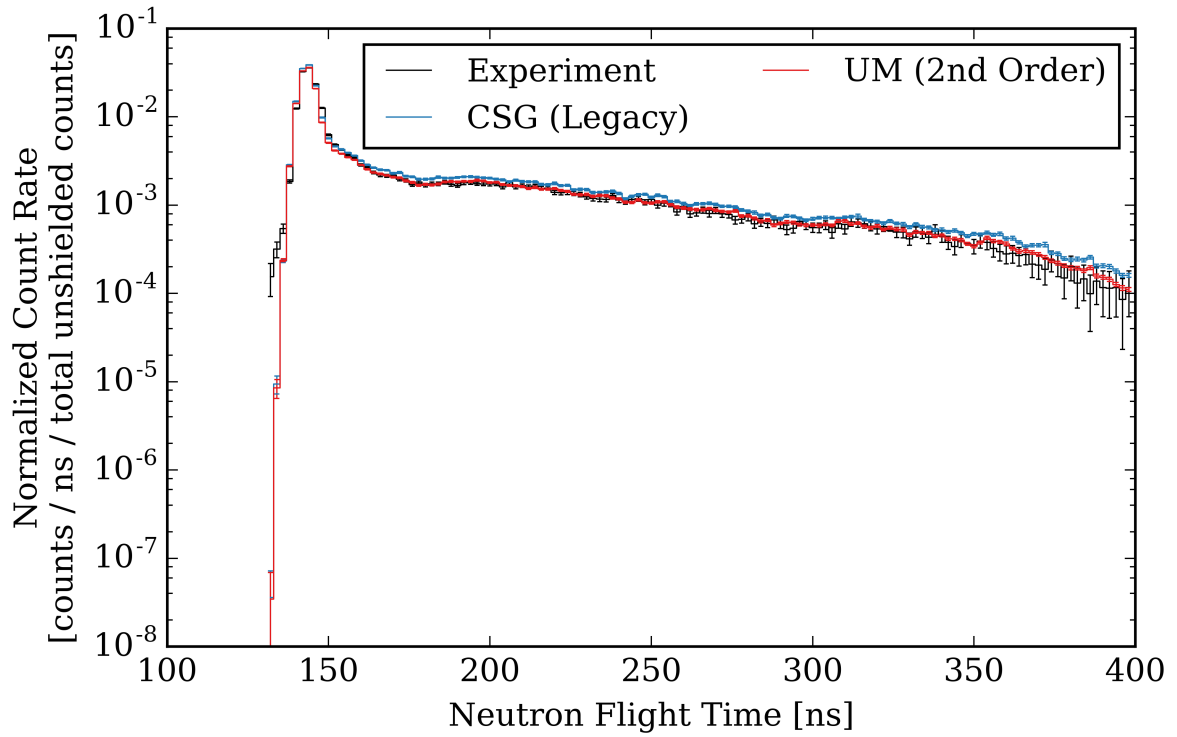
The Reference 8 work commented that the UM were generated finely enough to keep the masses within 1% for the spheres and within 2% for the water sphere's shell. It was expected that the second-order elements would be a better fit to the curved surfaces in these benchmarks. The surprising issue with this work was the large number of second-order tetrahedra that were needed to model the thin, inner, stainless steel shell for the water sphere. 143362 element were used in total for the water sphere with 107531 being tetrahedra. 93360 tetrahedra were needed for the inner shell. There were two issues that made the element count larger than expected:

1. Meshing in Abaqus (for LANL models) is traditionally done at the part level. For thin shells a higher element count is needed to minimize overlaps with other shells.
2. Without considerably more effort to segment the part that was the inner shell, only tetrahedra could be used in the meshing process. Using a maximum edge length that was too large resulted in elements with large aspect ratios and consequently distorted / deformed elements. The element checking capability of the *um_pre_op* utility [3] was used to verify that the second-order elements were acceptable. Tracking with distorted / deformed elements is not expected to work in MCNP6. If they are used, the code can hang. **Users should always perform this check before using a virgin mesh in MCNP6.**

From the evidence presented here (visual examination, χ^2 goodness-of-fit test, and fractional errors) it can be concluded that the pulsed sphere UM models adequately agree with the CSG and experimental results.



(a) Natural Beryllium



(b) Water

Figure 3: Pulsed Sphere Time-of-Flight Spectra for CSG and UM cases (all results include $\pm 1\sigma$ uncertainty bars).

Table 14: Fractional Errors for Pulsed Sphere Calculated Spectra Relative to Experimental Spectra

Experiment	CSG			UM
	Detailed	Hybrid	Legacy	
Beryllium	0.1358	0.1347	0.0585	0.0539
Water	0.0126	0.0134	0.0105	0.0085

Table 15: Fractional Errors for Pulsed Sphere Calculated Spectra (UM) Relative to CSG Legacy Spectra

Experiment	UM
Beryllium	0.0051
Water	0.0000

3.4 Simple Problem Results

A single history is used (because the problem is void) with an UM EMBEE4 (track length) edit. The EMBEE4 edit values for sources located at Q_1 and Q_2 are identical. The value from the edit for each UM element is multiplied by that element’s volume to determine the total track length deposited in each UM element. The element-by-element track lengths are then summed to determine the total track length deposited in the UM. When the track lengths from the lower two elements in Figure 2 are summed, the result is 1.86749 cm (with the top two elements each having zero track length). This agrees well with the analytic value (1.86894 cm) and therefore suggests that tracking is performed correctly. Furthermore, this shows that curvature can be reasonably well represented with a coarse second-order mesh seed. Re-meshing with a finer seed of 0.2 cm leads to a calculated track length of 1.86894 cm. The reason for this improvement is that second-order mesh permit curvature on the faces, but the finite element basis functions that define that curvature cannot exactly represent spheres/circles. This is because of the make up of the second-order basis (mapping) functions [2]. Thus, even with second-order elements it is still important to ensure that the UM is adequately refined for the application at hand.

4 Summary

This work has demonstrated that MCNP6’s revised second-order tracking routines on UM are working correctly and producing acceptable answers using four well-known benchmark problems and one new analytical benchmark. This demonstration is made with both fixed-source and eigenvalue calculations. Furthermore, the revised second-order tracking in code version 6.2.1 is much faster (by approximately a factor of 3–4) than the second-order tracking in previous code versions (6.1.4), but is still slower than tracking on first-order elements (by approximately a factor of 3) when the number of elements is held constant. Additional memory requirements when using second-order elements is modest—generally no more than a 25% increase. However, when far fewer elements (by approximately 100x less) are required, an overall memory savings can be achieved, which can be useful for very memory-intensive problems.

Calculations with first-order elements are faster and less memory intensive than with second-order elements. However, for comparable levels of detail (mass/volume preservation) and accu-

racy, approximately $100\times$ less second-order elements are needed which can lead to an overall memory savings and decreased calculation time. Accurately modeling volumes/masses is particularly important to obtaining the correct K_{eff} for kcode calculations. Because of the superiority of the second-order elements in this regard, care should be exercised when using first-order elements for eigenvalue calculations, particularly when there are parts with curved surfaces present.

Note that all meshes should be checked for deformed / distorted elements with `um_pre_op`'s element checking capability. This is particularly important when meshing thin shells.

Acknowledgements

Thanks to Joshua Spencer in helping with the SpaceClaim models for the LLNL pulsed sphere benchmarks.

References

- [1] R. L. Martz, "Preliminary Investigative Results of Mixed Geometry Models in MCNP with Some Benchmark Problems," April 2008.
- [2] R. L. Martz and D. L. Crane, "The MCNP6 Book On Unstructured Mesh Geometry: Foundations," Tech. Rep. LA-UR-12-25478 Rev 1, Los Alamos National Laboratory, Los Alamos National Laboratory, March 2014.
- [3] R. L. Martz, "The MCNP6 Book On Unstructured Mesh Geometry: User's Guide for MCNP 6.2," Tech. Rep. LA-UR-17-22442, Los Alamos National Laboratory, Los Alamos National Laboratory, March 2017.
- [4] "International Handbook of Evaluated Criticality Safety Benchmark Experiments," Tech. Rep. NEA/NSC/DOC(95)03/I-IX, Organization for Economic Co-operation and Development — Nuclear Energy Agency (OECD-NEA), Paris, France, September 2013.
- [5] C. Wong *et al.*, "Livermore Pulsed Sphere Program: Program Summary Through July 1971," Tech. Rep. UCRL-51144, Rev. 1, Lawrence Livermore National Laboratory, Livermore, CA, USA, 1972.
- [6] T. P. Burke *et al.*, "Reactor Physics Verification of the MCNP6 Unstructured Mesh Capability," in *International Conference on Mathematics and Computational Methods Applied to Nuclear Science & Engineering (M&C 2013)*, (Sun Valley, ID, USA, May 5–9, 2013), American Nuclear Society, 2013.
- [7] E. F. Plechaty and R. J. Howerton, "Calculational Models For LLL Pulsed Spheres (CSEWG Shielding Benchmark Collection No. SDT 10)," Tech. Rep. UCID-16372, Lawrence Livermore National Laboratory, Livermore, CA, USA, 1973.
- [8] J. A. Kulesza and R. L. Martz, "Evaluation of Pulsed Sphere Time-of-Flight and Neutron Attenuation Experimental Benchmarks Using MCNP6's Unstructured Mesh Capabilities," *Nuclear Technology*, vol. 195, pp. 44–54, July 2016.
- [9] Dassault Systèmes Simulia Corporation, "Abaqus/CAE 6.14 Online Documentation," 2014.

- [10] R. L. Martz, “An Unstructured Mesh Performance Assessment in the MCNP code Version 6.2,” Tech. Rep. LA-UR-17-27811, Los Alamos National Laboratory, Los Alamos, NM, USA, August 2017.
- [11] A. S. Bennett and B. C. Kiedrowski, “Revisiting the MCNP Shielding Validation Suite,” Tech. Rep. LA-UR-11-04540, Los Alamos National Laboratory, Los Alamos, NM, USA, 2011.